EVALUATION OF TRACTION CHARACTERISTICS OF TRACTOR TIRES ON LOOSE SOILS: SIMULATION AND EXPERIMENTAL RESEARCH
/
拖拉机轮胎在松软土壤上的牵引特性评价：仿真与试验研究

Jie WANG[1)], Lili SHANG[1)], Liangyuan XU[1,2)], Qiansheng TANG[1,2*)]
[1)] School of Engineering, Anhui Agricultural University, Hefei / China;
[2)] Anhui Intelligent Agricultural Machinery Equipment Engineering Laboratory, Hefei / China
E-mail: qiansh_tang@ahau.edu.cn
DOI: https://doi.org/10.35633/inmateh-71-33

Keywords: *bias-ply tire, tilled soil, Finite Element Analysis (FEA), traction characteristics*

ABSTRACT

In this study, a tire-soil rolling contact model based on the finite element method was established to determine the traction characteristics of the tire on the loose soil. Considering the soil parameters and tire parameters (loads, slip, inflation pressure and tread pattern), the influence of traction characteristics of the tire was obtained, taking tire sinkage and gross traction as evaluation indexes. The correctness of the tire-soil rolling contact model was verified by carrying out the soil bin-single wheel experiments. The results of the simulation and test showed that with the increase of load and sinkage of the tire, the gross traction tended to increase, thus enhancing the tire traction characteristics. With the increase of slip, the tire sinkage and gross traction increased, and the best tire traction characteristics were exhibited at a slip of 20%. Within the rated inflation pressure, as the inflation pressure increased, the tire sinkage decreased, the tire gross traction decreased and the traction characteristics of the tire were weakened. Under simulated working conditions, the traction characteristics of the tire first increased and then decreased with the increase of the number of tire lug pairs, and 15 tire lug pairs performed best. This paper presents a further study on the interaction between tires and soil under different influencing factors, and its findings provide an effective reference for predicting the traction performance assessment of tractor tires on working roads.

摘要

为了分析农用轮胎在松散土壤上的牵引特性，本研究以某型拖拉机轮胎为研究对象，综合考虑土壤参数、轮胎载荷、滑移、充气压力、胎面花纹等因素，以轮胎下沉量、轮胎总牵引力为指标来评价轮胎在土壤上的牵引性能。采用有限元方法建立了轮胎-土滚动接触模型，进行了轮胎-土沟槽试验。仿真与试验结果表明：随着载荷和轮胎下沉的增加，总牵引力呈增大趋势，从而增强了轮胎牵引特性。随着滑移量的增加，轮胎下沉量和总牵引力不断增大，在滑移量约为 20%时表现出最佳的轮胎牵引力特性。在额定充气压力范围内，随着充气压力的增大，轮胎下沉减小，总牵引力减小，轮胎的牵引力特性减弱。在模拟工况下，随着轮胎花纹数的增加，轮胎的牵引特性先增大后减小，存在最优值。本文深入研究了不同影响因素下轮胎与土壤的相互作用，其研究结果为预测拖拉机轮胎在工作道路上的牵引性能评估提供了有效参考。

INTRODUCTION

In recent years, an increasing number of large and medium-sized tractors have been used in agricultural production, and the rapid development and application of tractors have improved agricultural production efficiency to a certain extent. However, the increase in tractor power does not necessarily lead to an increase in production efficiency, since its driving ability also depends on the soil. The tire is the component in the closest contact with the soil, thus exploring the characteristics of the tire's movement on the soil is of great importance for improving the tire traction characteristics. The traction characteristics of tires on the soil have been investigated.

Wang et al. (2015) constructed a three-dimensional nonlinear finite element tire model with a detailed tread pattern and a smooth tread tire model for comparison. In these tire models, the tire-rim and tire-road interactions were considered and studied in the relationship between vertical loading and tire deflection, and the contact footprints, along with the pressure distribution achieved by the pressure-sensing pad experiment and the finite element tire modeling. *Sun et al. (2019)* established a finite element model for a 195/65R15 radial tire with the nonlinear analysis software ABAQUS, based on the tire structure and cord parameters.

[1] *Jie Wang, M.S. Stud. Eng; Lili Shang M.S. Stud. Eng; Qiansheng Tang, Ph.D. Eng.; Liangyuan Xu, Prof. Ph.D. Eng.*

Under constant tire pressure and load, the impact of velocity change on tire-cord stress during high-speed tire rolling was studied based on the finite element model to identify the relation between the cord stress and standing waves. *Wei et al. (2020)* proposed a finite element method for the analysis of the tire structure under the working conditions of assembly, with the help of ABAQUS software and the necessary evaluation of the finite element results of the loading condition, punching gas and loading, was also carried out. *Yamashita et al. (2018)* established a finite element model of wheel-soil interaction by using the multiplicative finite strain plasticity theory along with the capped Drucker-Prager failure criterion *(Drucker et al., 2013)*, investigated soil shaping, and analyzed the effects of tire-road friction, tire inflation pressure, vehicle velocity, and other factors on tire rolling radius and axle input torque.

Nakashima et al. (2009) analyzed the tractive performance of real automobile tires with two different tread patterns-smooth and grooved by FEA-DEM, to clarify the capabilities and limitations of the method for soil-tire interaction analysis. *El-Sayegh et al. (2020)* presented the coupling method of FEA-SPH to compute the interaction between an 8x4 off-road truck and gravelly soil (sand with gravel soil). The effect of gravelly soil compaction and truck loading on tire performance was discussed and investigated. *Zhao et al. (2019)* used the three-dimensional finite-discrete element method (FEM-DEM) for the simulation of tire-sand interactions, where the tire was discretized into hexahedron finite elements, and sand was modeled by using the discrete element method. *Zeng et al. (2019)* carried out the traction behavior research of an off-road tire on gravel terrain by the DEM-FEM coupling model with the calibrated microscopic input parameters mentioned.

Michael et al. (2015) proposed an efficient combination of the Discrete Element Method (DEM) and the Finite Element Method (FEM) to study the tractive performance of a rubber tire in interaction with granular terrain. *Bao et al. (2020)* analyzed the possibility of the wheels with wheel structure parameters and moving speed as experimental factors and designed a hydrostatic drive four-wheel vehicle. The values of wheel torque and rotational speed of each wheel in a wheel-soil contact simulation were confirmed to be consistent with actual values in the four-wheel vehicle. *Hu et al. (2021)* established an off-road tire steering model on sandy soil by using the discrete element method, the parameters of the sandy soil model were calibrated based on the triaxial compression test and inclined plate experiment. The influence of the steering radius, roll angle, and slip rate on the tire steering process was studied.

Huang et al. (2015) established a tractive trafficability predicted model through soil bin tests under light load, to study the tractive performance of lightweight vehicles on soft ground. Adopting the condition of light load with wheel load ranging from 30 to 90 N, the wheel sinkage, drawbar pull and tractive efficiency were taken as experimental indices, the wheel diameter, load and slip ratio were as experimental factors, and the regression orthogonal experiment scheme was designed. The effects of experimental factors on wheel tractive trafficability were also analyzed. Much literature focuses on rigid tires, sandy soils, and the strain behavior of soil, but relatively little on the comprehensive consideration of soil parameters, tire driving parameters, and the traction performance of bias-ply tires.

Therefore, this study focused on tractor tires and comprehensively took into consideration multiple factors related to tire forces and movement states, such as load, slip, inflation pressure, and the tire tread pattern to analyze the traction characteristics of agricultural tires on loose soil. In this paper, to address the above drawbacks, a new tractor tire-soil rolling contact finite element model is proposed, and simulation and experimental cases are investigated to verify the availability of the proposed model.

The main objectives of this paper were to (1) develop a tractor tire model and verify its correctness, (2) determine the physical parameters of loose soil, (3) establish a new finite element model of tire-soil contact, (4) construct soil bin-single wheel tester and analyze the influence of tire load, slip and inflation pressure on the traction characteristics of tractor tire, (5) investigate the influence of number of tread patterns on the traction characteristics of tractor tire by simulation further.

MATERIALS AND METHODS

Tire Modeling

An 11.2-24 8-ply rating bias-ply agricultural drive tire was simulated in this research. Considering the complex geometric structure of tires and rims, the tire-rim system was simplified into five parts including tread, belt plies, carcass, bead, and rim based on the requirements of tire structure and reliability. The tire design manual was used to obtain the tire-related parameters which were shown in Table 1. According to the tire parameters, a 3-dimensional (3D) model of the tire was constructed by using CATIA computer-aided design software (*Dassault Systèmes, Vélizy-Villacoublay, France*), as shown in Fig. 1.

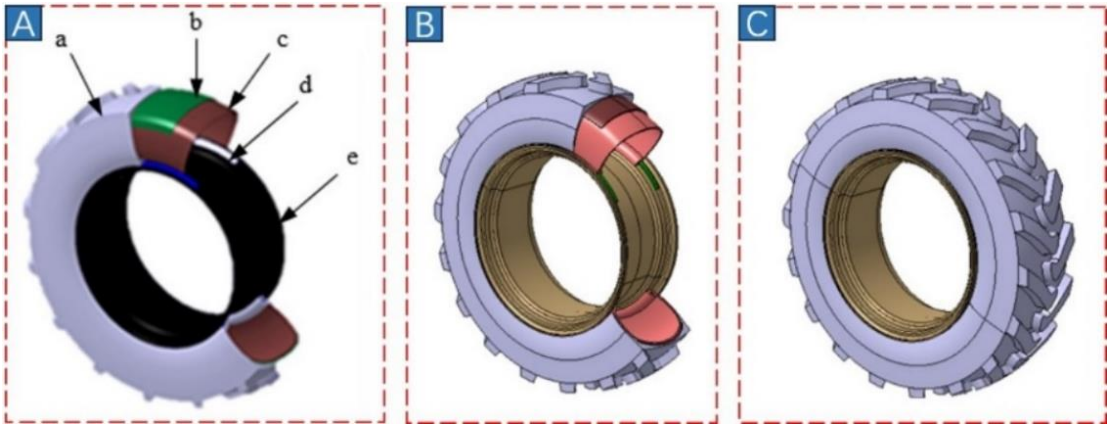

Fig. 1 – The tire 3D model

A is the structure of the tire schematic diagram (a – Tread; b – Belt ply; c – Carcass; d – Bead; e – Rim); B and C represent the tire 3D model in CATIA

Table 1

Tire-related parameters

Parameters	Overall diameter	Section width	Maximum inflation pressure	Maximum load
	[mm]	[mm]	[kPa]	[kg]
values	1105	285	240	1200

The 3D model of the tire was imported into the ANSYS Workbench finite element 118 analysis software (ANSYS, Inc., Canonsburg, PA), and correspondingly an appropriate material was assigned for each of the five tire components. Since the tread rubber material was highly non-linear and incompressible, the tread was simulated by the Yeoh constitutive model *(Li et al., 2016).* The carcass, Belt ply, and beads are the main load-bearing components of the tire. The materials of these tire components are composite materials that are composed of rubber materials and steel cords, and these tire components have the characteristics of anisotropic materials. Thus, these components were simulated with anisotropic materials in the process of modeling. The determined parameter values of the tread rubber material are shown in Table 2, and the defined parameter values of the tire carcass, Belt ply, and bead composite materials are shown in Table 3.

Table 2

Rubber material parameters

Component	Yeoh Material Ontology			Density (g/cm^3)
	C10	C20	C30	
Tread	2.3	-9.8	43.6	1.14

Table 3

Anisotropic material parameters

Parameters		Belt ply	Carcass	Bead
Density (g/cm^3)		1.11	1.14	7.8
Poisson's ratio	U_{xy}	0.0034	0.004	0.3
	U_{yz}	0.49	0.49	0.49
	U_{xz}	0.0034	0.004	0.3
Elastic modulus (MPa)	E_x	80641	24.3	281
	E_y	55.7	24.3	281
	E_z	55.7	6.01	64.4
Shear modulus (MPa)	G_{xy}	14.28	6.01	64.4
	G_{yz}	19.24	8.2	93.5
	G_{xz}	14.28	6.01	64.4

Validation of tire model

In the tire-soil contact model, the correctness of the tire finite element model affects the reliability of the simulation results of the tire rolling on the soil. To verify the correctness of the tire model, the finite element simulation of the tire was performed with an inflated simulated tire. The tire-rim system was modeled in ANSYS Workbench, and a simulated 240 kPa standard inflation pressure was applied to the inside of the tire.

When the tire was inflated, the tire was deformed in section direction and the overall diameter direction; the tire side-wall part expanded outward, and the tire crown part moved upward. The deformation degree of the tire crown was lower than that of the tire sidewall, which was due to the softness and easy deformability of the sidewall material. The tire inflation simulation is shown in Fig. 2. According to the tire design requirements, the tire model can be considered correct when the maximum tire section width and overall diameter are less than the values specified by the tire manufacturer. The results of the tire inflation simulations show that the tire was inflated to an overall diameter of 1111.2 mm and a section width of 303.8 mm, both of which were less than the maximum deformation size, as shown in Table 4. Thus, the finite element model of the tire established in this paper is reliable and can be used for subsequent steady-state rolling simulations of the tire on the soil.

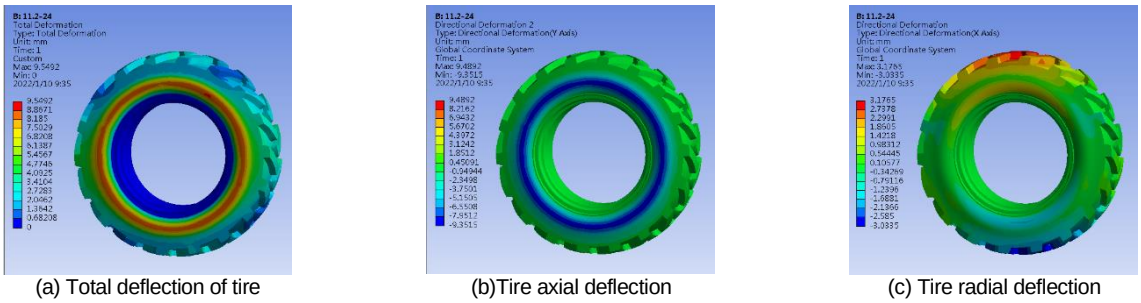

(a) Total deflection of tire (b)Tire axial deflection (c) Tire radial deflection

Fig. 2 - Tire deflections at the inflation pressure of 240 kPa (relative to standard atmospheric pressure)

Table 4

Tire inflation deformation volume compared with values specified by China National Standard (2017)

Dimension	After inflation simulation (mm)	Maximum allowable deformation after inflation (mm)
Overall diameter	1111.2	1135
Section width	303.8	308

Soil Modeling

The soil in contact with agricultural tires is mainly the soil at the plow layer (10 - 20 cm). The plow layer soil is affected by agricultural production activities, which makes the plow layer soil loose and unstable in physical properties. The mechanical properties of deep-layer soils with moderate water content and compact structure are hardly influenced by the external environment, thus deep-layer soil mechanical properties are excluded in this study. The modeling in this paper is based on the assumption that the soil is homogeneous, and the material of the soil is isotropic. In addition, in the process of modeling, the Drucker-Prager criterion is used to characterize the properties of soil materials. The Drucker-Prager criterion (DP criterion) is derived from the modification of the von Mises yield criterion, in which the yield strength-induced volume expansion is taken into consideration. DP criterion is expressed as follows (*Öztekin et al., 2016*):

$$\alpha I_1 + \sqrt{J_2} = K \tag{1}$$

where:

I_1 refers to the first invariant of the stress tensor; J_2 indicates the second invariant of the stress partial tensor; α and K are experimental parameters related to material properties and model selection, and they are determined by cohesion and internal friction angle. α and K are calculated according to the following formulae:

$$\alpha = \frac{2\sin\varphi}{\sqrt{3}\left(3-\sin\varphi\right)} \tag{2}$$

$$K = \frac{6C\cos\varphi}{\sqrt{3}\left(3-\sin\varphi\right)} \tag{3}$$

where: C is cohesion, (kPa); φ refers to angle of inter friction, (°).

The TSZ-2 full-automatic triaxial instrument (Nanjing soil instrument factory Co., LTD. China) was used in the triaxial experiment, which includes a pressure chamber, an axial compression system, a confining pressure loading system, and a software module.

The soil sample used in this experiment was yellow loose soil with a dry basis water content of 13.25% and the dry bulk density of 1.509 g/cm^3 (ρ). The diameter and height of the soil were 39.1 mm and 80 mm, respectively.

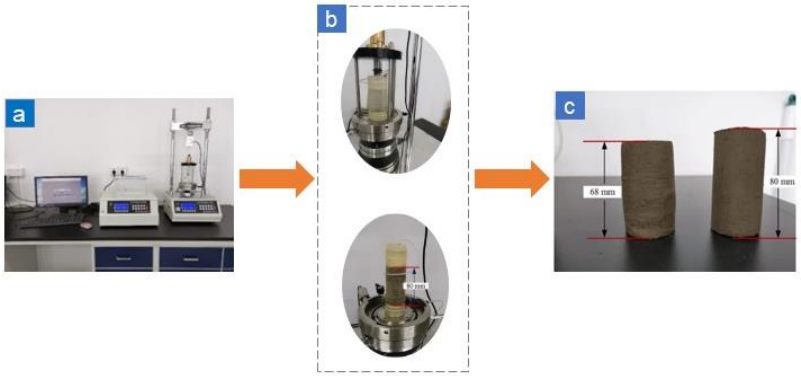

Fig. 3 - Soil triaxial instrument and deformation of soil sample at the end of the experiment

a – TSZ-2 full-automatic triaxial instrument; b –Soil loading; c – Experimental results.

In this paper, the mechanical properties of soil were measured by a triaxial experiment, and the process of the experiment is shown in Fig. 3. The experimental results are shown in Table 5.

Table 5

Loose soil parameters

Parameters	Density	Poisson's ratio	Shear modulus	Cohesion	Angle of internal friction
	[g/cm^3]	[%]	[MPa]	[kPa]	[°]
value	1.509	0.32	45	33.09	12.2

The wet bulk density and water content of undisturbed soil in the field were measured by using the cutting ring method on the samples from the surface layer (0 – 5 cm). To ensure the accuracy of the experiment, four measurement points were selected, among which three samples were taken from each point and the average value was taken as the measurement value of the point. The size and volume of the cutting ring in this experiment are Φ70×52 mm and 200 cm^3 respectively, as shown in Fig. 4. The wet bulk density of soil was obtained according to the following formulae:

$$\rho_0 = \frac{m_1 - m_2}{v} \tag{4}$$

where: ρ_0 is soil wet bulk density (g/cm^3), m_1 is the total weight of ring knife and soil, (g); m_2 is cutter weight, (g); v is ring cutter volume, (cm^3).

Fig. 4 - Soil wet bulk density and moisture determination experiment

a – Cutting ring; b – Self-weight of Aluminum box; c – Self-weight of soil; d – Weight of soil dried for 3 hours ; e – Drying oven; f – Constant weight of soil dried for 6 hours

The water content of the soil was obtained by drying the soil to constant weight in a drying oven, as shown in Fig. 4. The water content is then obtained according to the following formulae:

$$\omega = \frac{m_4 - m_5}{m_4 - m_3} \times 100\% \quad (5)$$

where:

ω is slip (per); m_3 refers to the self-weight of the Aluminum box (g); m_4 is the weight of soil and Aluminum box (g); m_5 indicates the constant weight of soil, (g).

The dry bulk weight of the field soil is then obtained according to the following formulae:

$$\rho = \frac{\rho_0}{1 + 0.01\omega} \quad (6)$$

where: ρ is dry bulk density of soil, (per).

The results of the density and water content experiment of the farmland soil are shown in Table 6:

Table 6

Test to get the bulk density and moisture content of farmland soil

Soil type	Measure point	Wet bulk density	Moisture content	Dry bulk density	Average wet bulk density	Average moisture content
		[g/cm³]	[%]	[g/cm³]	[g/cm³]	[%]
Loose soil	1	1.492	13.5	1.315	1.509	13.25
	2	1.504	13.3	1.327		
	3	1.523	13.4	1.343		
	4	1.515	12.8	1.343		

Tire-soil Contact Modeling

A tilled soil model was constructed with a length of 5 m, a width of 1 m, and a height of 0.8 m by using CATIA software. In terms of the characteristics of loose and soft soil, the soil was divided into two layers, namely, the tilled layer soil and the base layer. Based on the results of the triaxial experiment, the material parameters of the soil were added to ANSYS Workbench to determine the relevant parameters of the loose soil.

The establishment of the tire-soil contact model is the basis for the analysis of the interaction between the tire and the soil, and the contact state between the tire and the soil has a significant impact on the traction characteristics of the tire. In this study, a tire-soil rolling contact model was established by CATIA software (see Fig. 5A) and imported into ANSYS Workbench for simulation.

In this study, the tire sinkage, and gross traction were used as indexes to evaluate the traction characteristics of tires under the state of tire steadily rolling on the soil. The related indexes were calculated according to the following equations *(Zeng et al., 2019)*:

$$s = \frac{\omega r - v}{\omega r} \times 100\% \quad (7)$$

$$G_T = \frac{T}{r} \quad (8)$$

where: s is slip, (per); r refers to tire torque radius, (m); v is tire velocity, (m/s); T indicates input torque, (Nm); G_T is gross traction, (N).

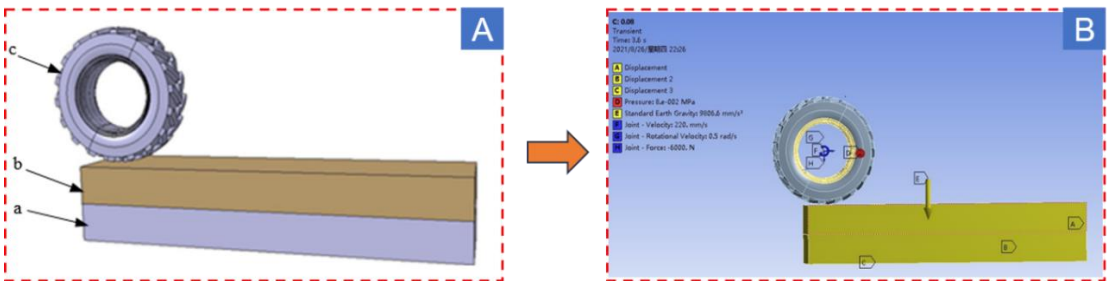

Fig. 5 - The tire-soil rolling contact model

a - The base layer; b -The tilled layer; c - Bias-ply tire

Firstly, the inflation pressure was applied to the tire in 0.02-0.34 s, and then the corresponding load was applied to the tire in 0.34-0.36 s. After the load on the wheel reached the target value, the tire was loaded with angular and horizontal velocity in 0.36-0.54 s. The simulation was performed by fixing the tire's angular velocity and changing the horizontal velocity of the tire to obtain different slips. The tire sinkage and tire traction were obtained by post-processing the simulation results, and the tire traction performance was studied by analyzing the results of the data on tire sinkage and tire gross traction (displacement was 0 mm, inflation pressure of tire was 8 kPa, the vertical load here was 6 kN). The tire-soil rolling contact model was shown in Fig. 5B. The mesh size in the tire-soil rolling contact simulation model was shown in Table 7.

Table 7

Mesh sizes used in the FEA model

Component	Tread	Belt ply	Carcass	Bead	Soil
Mesh size (mm)	32	32	32	28	20

A soil bin-single wheel tester composed of a soil bin, a single wheel test device, and a control and data acquisition system, was built to verify the accuracy of the numerical simulation results. The tire was mounted on the tire drive shaft of the soil bin tester. Firstly, a vertical load was applied to the tire and the magnitude of the vertical load was measured to a specified value by using a load cell and a screw jack. Secondly, the frequency conversion motor and servo motor were activated to pull the single wheel carriage assembly along the direction of travel to the specified speed with the tire being free-rolling, ensuring that the tire enters a stable driving state under a certain load. During the driving process, the torque sensor and the wire displacement sensor were used to record the values of the traction torque and sinkage of the tire, respectively. Then, the experiment curve of the traction torque and sinkage of the tire were obtained by using these values. Finally, the resultant values for the steady rolling condition of the tire were taken as the traction torque and sinkage of the tire under this load for subsequent calculations. The soil bin-single wheel tester was shown in Fig. 6.

Fig. 6 - Soil bin-single wheel tester

(a) Displacement sensors for the value of sinkage of the tire acquisition (b) Jack and load sensors (c) Laptop computer for data acquisition (d) Wheel input torque sensor (e) Traction motor unit to drive the wheel axle

RESULTS

Effect of Load

Because the soil resistance to the thrust and rolling of the tire is affected by the load on the tire, the traction characteristics of the tire are related to the load on the wheel. To explore the influence of on-wheel load on the traction characteristics of tire-soil contact, six groups of different on-wheel loads were simulated at a fixed slip rate of 20% and constant inflation pressure of 240 kPa. The six on-wheel load values were 0, 2000N, 4000 N, 6000 N, 8000 N, and 10000 N, respectively.

The cloud images of tire rutting imprint after the tire rolled under different loads were shown in Fig. 7, and the tire sinkage curve and traction curve were shown in Fig. 8. With the load on the wheel, the more obvious the rutting mark of the tire, the greater the soil deformation.

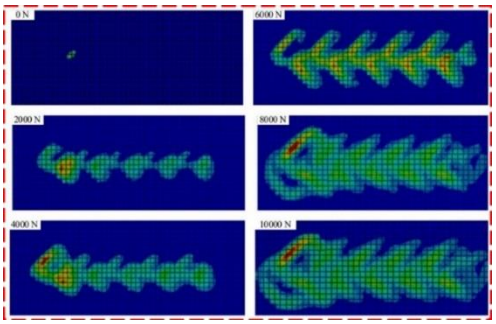

Fig. 7 - Comparison of tire rutting marks under different loads

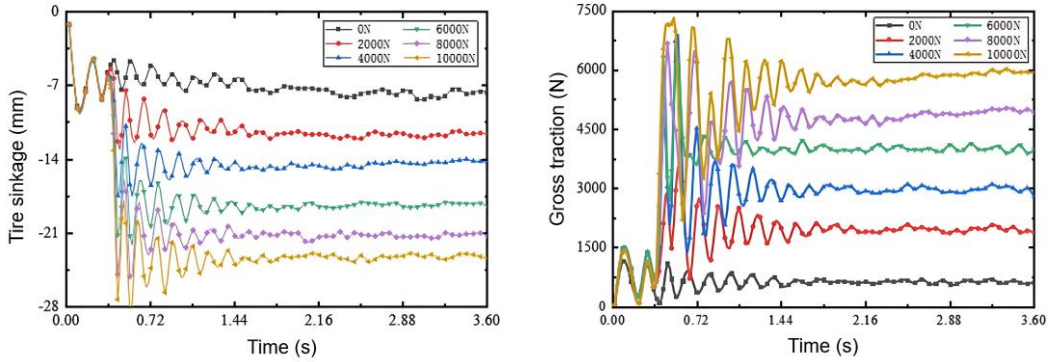

(a) Tire sinkage curve (b) Gross traction curve

Fig. 8 - The curve of the effect of different loads on the tire-soil contact action

In Fig. 8a and Fig. 8b, the tire was in the state of inflation, on-wheel loading, and speed loading during the first 0.54 s at the beginning of the simulation, and after 0.54 s, the tire was loaded to the corresponding horizontal speed and rotation speed. Due to the material nonlinearity of the tire and the soil, the geometric nonlinearity caused by the tire and soil deformation, and the contact nonlinearity during the rolling process, the corresponding values of variables such as sinkage and gross traction fluctuate, and then gradually become stable. The corresponding simulation results were obtained when the tire sinkage and gross traction values became stable during the tire rolling process. The relationship among tire sinkage, gross traction, and tire load was presented in Fig. 11.

As shown in Fig. 9a, the tire sinkage simulation value increased from 7.3 mm to 23.9 mm with the increase in tire load. In Fig. 9b, the tire gross traction simulation value increased 9.02 times with the increase in tire load. These results could be explained as follows: with the increase of tire load, the normal force of the tire on the soil increased, thus resulting in larger soil sinkage and a larger contact area between the tire and soil. In the case of the fixed ground adhesion coefficient, the larger the tangential reaction force of the soil on the tire, the larger the tire's gross traction, and the better the traction characteristics.

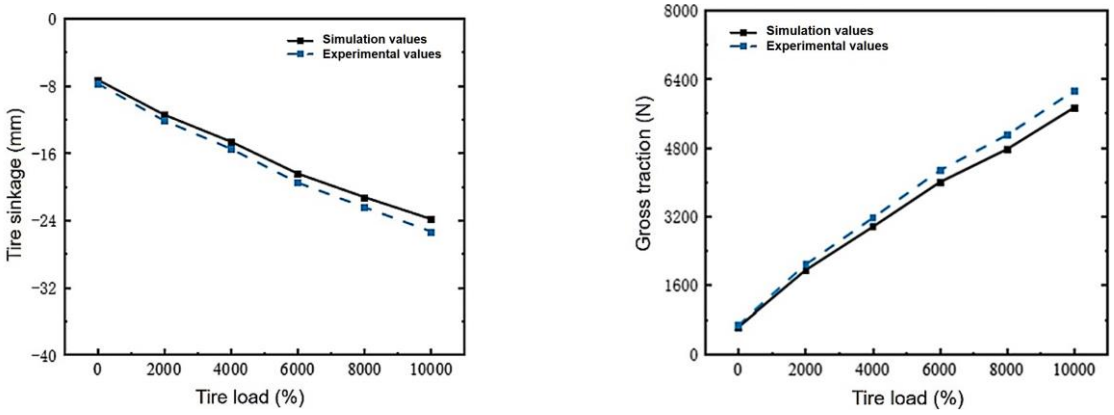

(a) Tire sinkage (b) Gross traction curve

Fig. 9 - Effect of different loads on tire-soil contact interaction

Effect of Slip

The tire slip affects the shear deformation of soil and tire-soil contact surface, thereby affecting the tire traction characteristics. In this study, the tire slips were set as 5%, 10%, 15%, 20%, 25%, and 30%, respectively at a tire load of 6000 N and tire inflation pressure of 240 kPa. After the steady-state rolling results were processed, the values of tire sinkage, and tire gross traction under different tire slips were obtained to reveal the influence of different tire slips on tire traction characteristics (Fig. 10).

As shown in Fig. 10a, with the increase of the slip, the tire sinkage simulation value was firstly continuously increased, reaching the value of 18.47 mm at about 20% of the slip, and then the rate of growth tended to be stable. The gross traction increased as the slip increased, but there was a clear turning point for growth. As shown in Fig. 10b, when the slip increased from 5% to 20%, the increase in gross traction was greater; the trend in gross traction flattened out as the slip increased from 20% to 30%. When the slip reached 20%, the gross traction growth rate turned around indicating that the optimal tire traction characteristics were obtained.

As a result of the increase in slip, the shearing effect of the tire on the soil is enhanced, thus resulting in the enlarged soil shearing deformation and the increased tire sinkage. During the tire slipping process, the compaction of the soil is increased, thus soil deformation is reduced, and the tire sinkage is no longer increased. With the increase of slip, the soil is sheared to produce stacking. To ensure the normal driving of tires, tire gross traction is increased. When the tire slip intensifies to a certain extent, the soil compaction increases, and the shear force acting on the soil reaches the maximum and is limited by soil adhesion, thus the tire gross traction gradually becomes stable.

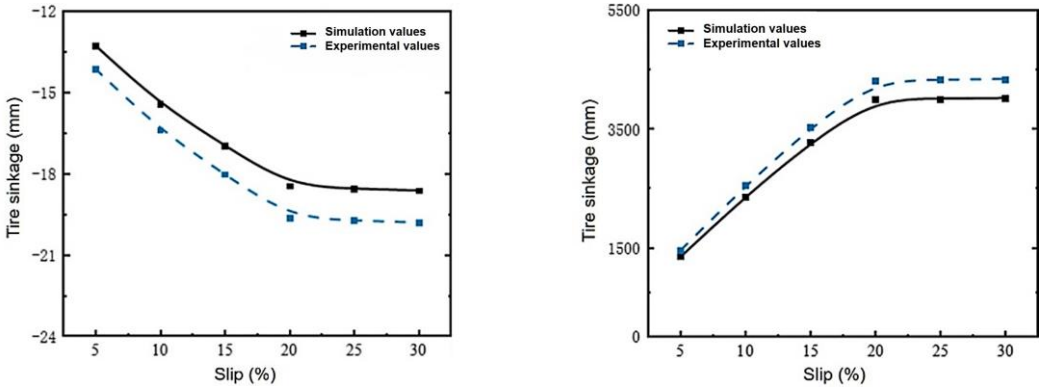

(a) Tire sinkage (b) Variation of gross traction

Fig. 10 - Effect of different slip on tire-soil contact interaction

Effect of Inflation Pressure

The change in the tire inflation pressure affects the stiffness of the tire which affects the adhesion of the tire to the soil. At the fixed tire slip of 20% and tire load of 6000 N, the influence of tire inflation pressure on tire traction characteristics was investigated under the inflation pressure conditions of 80 kPa, 120 kPa, 160 kPa, 200 kPa, and 240 kPa, respectively.

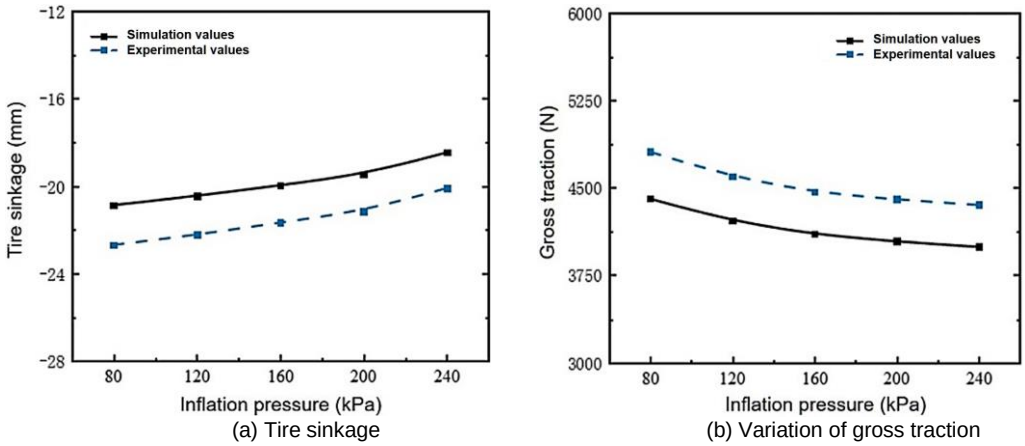

(a) Tire sinkage (b) Variation of gross traction

Fig. 11 - Effect of different inflation pressures on tire-soil contact interaction

As shown in Fig.11a, within the rated inflation pressure range (80 ~ 240 kPa), the sinkage of the tire decreases with the increase of inflation pressure, and when the rated inflation pressure reaches the maximum (240 kPa), the tire sinkage simulation value reaches a minimum of -18.47 mm. In Fig.11b, tire gross traction gradually decreases with the increase of tire inflation pressure, and the rate of gross traction reduction gradually decreases. When the inflation pressure reaches its maximum (240 kPa), the gross traction of the tire reduces by 8.5%.

With the increase of inflation pressure, the tread gradually deformed, the tire sidewall and crown parts expanded outward under the inflation pressure, and the tire stiffness increased. Under the same load, the contact area between the tread and soil under high inflation pressure was smaller than that under low inflation pressure, thus leading to the weakened shearing and compaction effects of tires on soil, eventually resulting in the decrease of tire sinkage and tire gross traction. Therefore, when the tractor works on the agricultural soil surface, the tire pressure should be reduced appropriately to improve the tire traction characteristics.

Effect of Number of pairs of lugs on the tire

The number of tread patterns affects the tire tread gap and the contact area between the tire and the soil. To investigate the effect of the contact area between tread and soil on tire traction characteristics, the finite element software was used to analyze the influence of the number of tread patterns on the traction characteristics of the tire, based on the traction characteristics under tire load, slip rate, and tire pressure that has been verified experimentally. The number of pairs of lugs on the tire was used to characterize the gap among tire patterns and tire-soil contact area, with the constant size of lugs on the tire. At the fixed tire slip of 20%, an inflation pressure of 240 kPa, and a constant wheel load of 6000 N, the effects of tire patterns on the tire sinkage, and tire gross traction were investigated by changing the number of pairs of lugs on the tire. (Fig. 12).

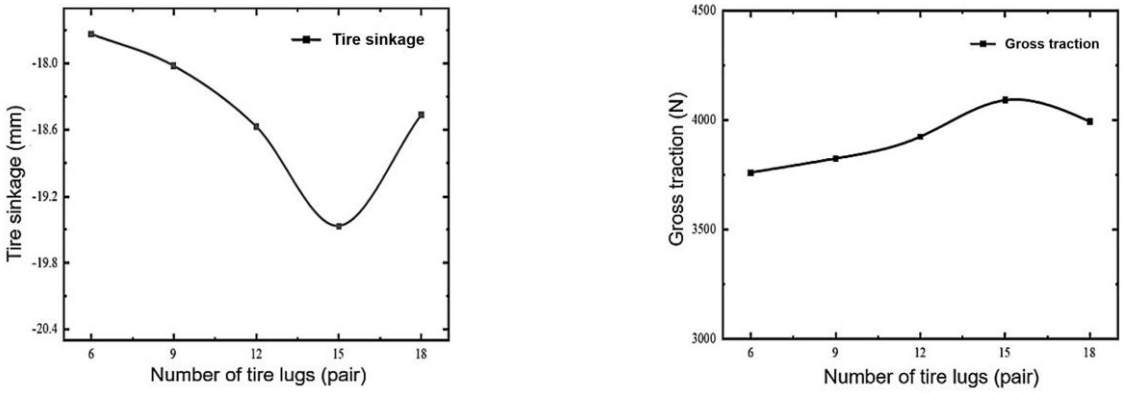

(a) Tire sinkage amount (b) Variation of gross traction

Fig. 12 - Effect of different tread densities on tire-soil contact interaction from simulation

As shown in Fig. 12a, the tire sinkage increases with the increase of the number of tire lug pairs. The tire sinkage reaches the maximum of -19.47 mm when the number of pairs of lugs on the tire increases to 15, and thereafter the tire sinkage decreases with the increase of the number of tire lug pairs. As shown in Fig. 12b, the gross traction force firstly increases and then decreases as the number of lug pairs increases. When the number of tire lug pairs increases to 15, the tire gross traction reaches the maximum of 4091 N, then the gross traction keeps decreasing.

Within a certain range, as the number of tire lug pairs increases, which results in the enhancement of the cutting effect on the soil and the increase of the shear slip surface, the soil sinkage and the gross traction increase, namely the enhancement of the traction characteristics of the tire. However, the excessive number of pairs of lugs on the tire will lead to a decrease in the gap between tread patterns, thus the tire gradually turns into a glossy tire, thereby weakening the shear effect of the tire on soil, namely, reducing gross traction to adversely affect tire traction characteristics.

The research content of this paper provides an effective reference value for the analysis of tractor tire-soil interaction using the finite element method. Its findings provide an effective reference for predicting the traction performance assessment of tractor tires on working roads.

CONCLUSIONS

In this study, a tire-soil rolling contact model was constructed using the finite element method, the tire-soil groove experiments were carried out, and the traction characteristics of the tire were analyzed based on multiple influencing factors such as the load, the slip, the inflation pressure, and the number of pairs of lugs on the tire.

The major conclusions were as follows:

(1) With the increase in on-wheel load, and the tire sinkage, gross traction showed an increasing trend, thus enhancing the traction characteristics.

(2) With the increase in the slip, the tire sinkage and the gross traction were continuously increased, reaching the growth rate turning point at the slip of about 20%, exhibiting the optimal tire traction characteristics.

(3) Within the rated inflation pressure range, as inflation pressure increased, the tire sinkage, and the gross traction decreased, thus the tire traction characteristics were weakened.

(4) Under the simulation conditions, with the increase of the number of tire lug pairs, the traction characteristics of the tire gradually increased and reached the maximum when the number of tire lug pairs was 15, and afterward decreased, thus 15 tire lug pairs performed best.

The research content of this paper provides an effective reference value for the analysis of tractor tire-soil interaction by using the finite element method. Its findings provide an effective reference for predicting the traction performance assessment of tractor tires on working roads.

ACKNOWLEDGEMENT

The authors thank Fund Project: National Key Research and Development Program and Technology Major Special Project and Anhui Province Engineering Laboratory of Intelligent Agricultural Machinery and Equipment and Anhui Agricultural University for their funding support.

REFERENCES

[1] Bao, Y. D., Yang, J., Zhao, Y. L., Liu, X. L., Guo, Y. L., Li, Z. P., & Xiang, J. Z. (2020). Design of the walking driving system for a blueberry harvester based on contact mechanical behavior of wheel-soil. *Transactions of the Chinese Society of Agricultural Engineering, China,* 36(07), 43-52. https://doi.org/10.11975/j.issn.1002-6819.2020.07.005

[2] Drucker, D. C., & Prager, W. (2013). Soil mechanics and plastic analysis or limit design. *q.appl.math, USA*, *10(2)*, 157-65. https://doi.org/10.1090/qam/48291

[3] El-Sayegh, Z., El-Gindy, M., Johansson, I., & Öljer, F. (2020). Development and validation of off-road tire-gravelly soil interaction using advanced computational techniques. *Journal of Terramechanics, Netherlands,* 91, 45-51. https://doi.org/10.1016/j.jterra.2020.05.004

[4] Hu, C., Gao, J., Diao, J., & Song, X. (2021). Numerical simulation of tire steering on sandy soil based on discrete element method. *AIP Advances, USA,* 11(1), 015015. https://doi.org/10.1063/5.0034585

[5] Huang, H., Li, J. Q., Wu, B. G., Zhang, G. Q., Xue, L., & Wang, Y. (2015). Construction and verification of lightweight vehicle wheel tractive trafficability model under light load. *Transactions of the Chinese Society of Agricultural Engineering, China,* 31(12), 64-70. https://doi.org/10.11975/j.issn.1002-6819.2015.12.009

[6] Michael, M., Vogel, F., & Peters., B. (2015). Dem–FEM coupling simulations of the interactions between a tire tread and granular terrain. *Computer Methods in Applied Mechanics and Engineering, Netherlands,* 289, 227-248. https://doi.org/10.1016/j.cma.2015.02.014

[7] Nakashima, H., Takatsu, Y., Shinone, H., Matsukawa, H., & Kasetani, T. (2009). FE-DEM analysis of the effect of tread pattern on the tractive performance of tires operating on sand. *Journal of Mechanical Systems for Transportation & Logistics, China,* 2(1), 55-65. https://doi.org/10.1299/jmtl.2.55

[8] Öztekin, E., Pul, S., & Hüsem, M. (2016). Experimental determination of Drucker-Prager yield criterion parameters for normal and high strength concretes under triaxial compression. *Construction and Building Materials, Netherlands, 112,* 725-732. https://doi.org/10.1016/j.conbuildmat.2016.02.127

[9] Sun, P. F., Huang, H. W., Zhou, S. T., Chiu, Y. J., Du, M., & Zhao, D. H. (2019). Experiment and analysis of cord stress on high-speed radial tire standing waves. *Shock and Vibration. USA*. https://doi.org/10.1155/2019/3607670

[10] Wang, W., Yan, S., & Zhao, Y. (2015). Numerical and experimental studies of a radial truck tire with tread pattern. *Simulation Transactions of the Society for Modeling & Simulation International, USA,* 91(11). https://doi.org/10.1177/0037549715608434

[11] Wei, L. J., Liu, H. O., Chen, H. Y., & Zhao, Z. Y. (2020). Finite element analysis of cross section of TBR tire. *Mechanics of Advanced Materials and Structures, USA,* 27(17). 1509-1517. https://doi.org/10.1080/15376494.2018.1517911

[12] Li, X. B., & Wei, Y. T. (2016). An improved Yeoh constitutive model for hyperelastic material. *Engineering Mechanics, China,* 33(12), 38-43. https://doi.org/10.6052/j.issn.1000-4750.2015.05.0388

[13] Yamashita, H., Jayakumar, P., Alsaleh, M., & Sugiyama, H. (2018). Physics-based deformable tire-soil interaction model for off-road mobility simulation and experimental validation. *Journal of Computational and Nonlinear Dynamics, USA,* 13(2), 021002. https://doi.org/10.1115/1.4037994

[14] Zhao, C. L., & Zang, M. Y. (2017). Application of the FEM/DEM and alternately moving road method to the simulation of tire-sand interactions. *Journal of Terramechanics, Netherlands,* 72, 27-38. https://doi.org/10.1016/j.jterra.2017.04.001

[15] Zeng, H. Y., Xu, W., Zang, M. Y., & Yang, P. (2019). Calibration of DEM-FEM model parameters for traction performance analysis of an off-road tire on gravel terrain. *Powder Technology, Netherlands,* 362, 350-361. https://doi.org/10.1016/j.powtec.2019.12.006